

## Beta-decay study of $^{101}\text{Cd}$

*Marta Polettini<sup>1,2,3,4,\*</sup>, Guangxin Zhang<sup>1,2,5</sup>, Giovanna Benzoni<sup>4</sup>, Daniele Mengoni<sup>1,2</sup>, Cenxi Yuan<sup>5</sup>, and the **HISPEC-DESPEC collaboration for the S496 experiment***

<sup>1</sup>Università degli Studi di Padova, Padova 35131, Italy

<sup>2</sup>INFN Sezione di Padova, Padova 35131, Italy

<sup>3</sup>Università degli Studi di Milano, Milano 20133, Italy

<sup>4</sup>INFN Sezione di Milano, Milano 20133, Italy

<sup>5</sup>Sino-French Institute of Nuclear Engineering and Technology, Sun Yat-Sen University, Zhuhai 519082, Guangdong, China

**Abstract.** This work reports on new experimental information regarding the beta decay  $^{101}\text{In} \rightarrow ^{101}\text{Cd}$ , obtained with the DESPEC set-up within the FAIR Phase-0 [campaign in the year 2021](#). A first tentative assignment of  $I_\beta$  and  $\log ft$  values is provided. The results are compared to large-scale shell-model calculations confirming the picture of allowed decays. The spin-parity of the added levels, assigned in previous fusion-evaporation experiments, is confirmed on the basis of decay feeding arguments.

### 1 Introduction

The region of the nuclide chart around  $^{100}\text{Sn}$  has been the subject of a multitude of experimental and theoretical studies in recent years. Specific efforts have been directed towards assessing the robustness of the  $N=50$  and  $Z=50$  double shell closure and the evolution of single-particle energies. In addition, the long isotopic chains with  $Z \sim 50$  serve as good testing grounds for nuclear models investigating the shell evolution and the interplay between pairing and quadrupole correlations.

This region is also ideal for studies of the evolution of the seniority symmetry, [established for these nuclei for a configuration of  \$n\$  protons in the  \$g\_{9/2}\$  orbit](#). Deviations emerge from the mixing with close-by orbitals [and from the effect](#) of core-excitations across the gap.

Unlike the case of Sn, where the generalized seniority scheme with neutron configurations [can be expected to hold for low-lying](#) states, understanding the Cd isotopic chain is more challenging due to the enhancement of collectivity induced by two proton holes in the  $g_{9/2}$  orbit.

The difference between neighbouring isotopic chains is reflected in the trend of  $2^+$  energies: the  $E(2_1^+)$  [in the Pd, Te and Xe isotopic chains gradually](#) increases with the neutron number towards  $N = 82$ , implying a smooth structural evolution from vibrational nature to a spherical shape. However, the situation in Cd isotopes is unusual: the  $2_1^+$  energy is rather constant, followed by a sudden increase in excitation energy in  $^{130}\text{Cd}$ , indicating a different shape evolution with respect to nearby isotopes [1].

\* e-mail: m.polettini@gsi.de  
Presently at GSI Helmholtzzentrum für Schwerionenforschung, Darmstadt 64291, Germany

Experimental data covering low- and high-spin states along the Cd isotopic chain from N=50 to N=82 was collected in recent years [2], typically using fusion-evaporation experiments and isomer-delayed  $\gamma$ -ray spectroscopy. Proton-rich Cd isotopes have been recently revisited on the basis of the study of proton or  $\beta$ -delayed proton emission, with the refinement of [half-life measurements](#) [3]. In addition, collinear laser spectroscopy data fixed spins and parities of the odd members of [the chain between](#) A=101-109, confirming a  $J^\pi=5/2^+$  ground state [4]. The electromagnetic moments in the mentioned isotopes, [compared to large-scale shell-model calculations](#) using the SR88MHJM Hamiltonian, firmly establish the significance of the  $\pi g_{9/2}$  contribution, and the importance of the joined filling of the close-lying  $d_{5/2}$  and  $g_{7/2}$  orbitals, for the observed nuclear structure. The level scheme of p-rich Cd isotopes was constructed in previous works on the basis of fusion-evaporation reactions, and was well assessed up to high spins. Beta decay can provide complementary information on the daughter nucleus, and offers an insight into non-yrast bands.

## 2 The experiment

The experiment was performed by the [HISPEC-DESPEC collaboration at GSI-FAIR in May 2021](#), as a part of the FAIR Phase-0 campaign. The ions of interest were produced in relativistic in-flight fragmentation reactions of a  $^{124}\text{Xe}$  beam on a  $^9\text{Be}$  target. The GSI accelerator complex provided a pulsed beam of 2s on/2s off,  $\sim 10^9$  pps intensity and an energy of 840 MeV/u. The ions in the produced cocktail beam were selected using the FRS Fragment Separator [5] using the  $B\rho - \Delta E - B\rho$  method and identified [thanks to the TOF -  \$B\rho - \Delta E\$](#)  method [6].

The species of [interest were transported](#) towards the DESPEC (DEcay SPECtroscopy) [7] implantation and decay station, located at the final focal plane of the FRS. Here, [ions were implanted in](#) a stack of two  $24 \times 8 \text{ cm}^2$  layers of Double-Sided Silicon-strip Detectors (DSSD), the AIDA set-up (Advanced Implantation Detector Array) [8] [where they subsequently decayed](#), sandwiched between two plastic scintillators. In this setup, AIDA is used to detect both implanted ions and  $\beta$  particles emitted following ion decay. The implantation [stack was surrounded](#) by a hybrid array of four 7-fold EUROBALL HPGe clusters [9] and 36  $\text{LaBr}_3(\text{Ce})$  detectors of the [FATIMA-FAst TIMing Array](#) [10], to measure the  $\gamma$  rays emitted in the de-excitation of the daughter nuclei.

The decay scheme of  $^{101}\text{Cd}$  has been studied via the  $\beta$  decay of the parent nucleus  $^{101}\text{In}$ , using  $\gamma$ - $\gamma$  correlations and intensity measurements in the single germanium energy spectra. The  $\beta$ -decay HPGe spectrum is obtained by measuring out of spill, in coincidence with the  $\beta$ -plastic scintillator detectors.

## 3 Results and discussion

The level scheme of  $^{101}\text{Cd}$  was previously studied with the  $^{58}\text{Ni}(^{50}\text{Cr},2p\alpha n)^{101}\text{Cd}$  fusion evaporation reaction using the NORDBALL array [11]. A beta decay study of the same nucleus was reported in Ref. [12], where only the first excited state at 253 keV could be placed in the level scheme.

In our experimental study, we have reconstructed [the decay scheme of](#)  $^{101}\text{Cd}$  from the beta decay of  $^{101}\text{In}$  by analysing gamma-ray spectra out of spill. Our study extends the knowledge on  $\beta$ -delayed  $\gamma$ -ray transitions in this nucleus, with the addition of two levels to the  $\beta$ -delayed level scheme and a first measurement of  $I_\beta$  and  $\log ft$  values.

$J_i^\pi \rightarrow J_f^\pi$	$E_x$ (keV)	$E_\gamma$ (keV)	EM character	ICC	$I_\gamma$ (%)
$7/2^+ \rightarrow 5/2^+$	252.9(5)	252.9(5)	$M1 + E2$	0.048(11)	100(4)
$9/2^+ \rightarrow 7/2^+$	891.9(5)	640.4(5)	$M1 + E2$	0.0036(2)	5(2)
$9/2^+ \rightarrow 5/2^+$	891.9(5)	891.9(5)	$E2$	0.00148(2)	49(3)
$11/2^+ \rightarrow 7/2^+$	1144.5(5)	891.9(5)	$E2$	0.00148(2)	16(3)

**Table 1.**  $\gamma$ -ray transitions assigned to  $^{101}\text{Cd}$ . The following quantities are listed: the spin-parity of initial ( $J_i^\pi$ ) and final ( $J_f^\pi$ ) states, the energy of the initial level ( $E_x$ ), the energy of the  $\gamma$  ray ( $E_\gamma$ ), its electromagnetic character, its internal conversion coefficient (ICC) and its relative  $\gamma$  intensity ( $I_\gamma$ ). The relative  $\gamma$  intensities for the 640- and 892-keV transitions are rescaled based on gamma-gamma coincidences

In Fig. 1, the  $\gamma$ - $\gamma$  coincidence transitions are shown. In the left panel, the 640- and 892-keV transitions are observed in coincidence with the 253 keV  $\gamma$  transition. In the right panel, the 253- is observed in coincidence with the 892-keV transition.

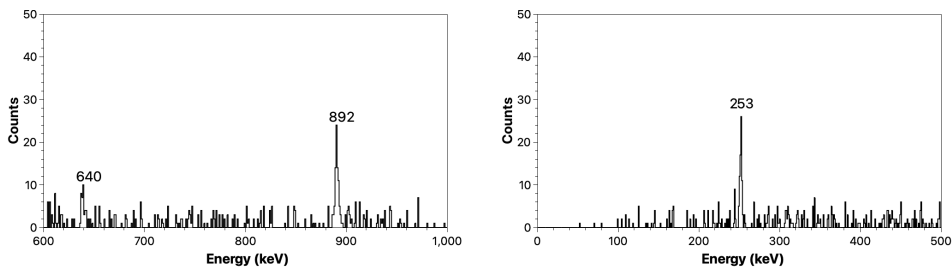


**Figure 1.** Gamma-ray spectra in coincidence with the 253 keV (left panel) and 892 keV transition (right panel).

The measured  $\gamma$  transitions are reported in Tab. 1, extracted from germanium singles spectra. The measured  $\gamma$  transitions are reported in Tab. 1, extracted from germanium singles spectra. The value of the relative intensity for the 639-keV and 891-keV transition, the latter being a doublet in the previously-proposed level scheme, was extracted via gamma-gamma coincidences. The intensities have been rescaled to that of the 253-keV transition, used as reference. Internal conversion coefficients for the given  $\gamma$  transitions, accounting for negligible contribution, were calculated using the BrICC online calculator [13].

In Tab. 2, the  $\beta$  intensities and  $\log ft$  values for the measured levels are listed. The  $\beta$  feedings ( $I_\beta$ ) were calculated by subtracting the gamma intensities ( $I_\gamma$ ) of the transitions feeding the level from the ones depopulating the level itself:  $I_\beta = I_\gamma^{(out)} - I_\gamma^{(in)}$ , divided by the total measured beta feeding. The  $\beta$  feedings for each level were used to extract the  $\log ft$  value, using the online tool provided by the NNDC website [14]. In this work, the  $I_\beta$  and  $\log ft$  values given are referred to  $\beta+$  and EC decays altogether, as the two contributions cannot be distinguished. The  $Q$ -value used for the extraction of  $\log ft$  values in this work was calculated considering the mass  $^{101}\text{In}$  reported in a recent publication [15]), obtaining the value  $Q = 7291(5)$  keV. The  $^{101}\text{In}$   $\beta$ -decay half-life considered is a weighted value between Ref. [12] and [16], and amounts to  $T_{1/2} = 15.1(3)$  s.

The results are compared to theoretical predictions, obtained using Large-Scale Shell Model calculations in the model space jj4\_45, including proton  $0f_{5/2}$ ,  $1p_{3/2}$ ,  $1p_{1/2}$ ,  $0g_{9/2}$  orbitals and neutron orbitals  $0f_{5/2}$ ,  $1p_{3/2}$ ,  $1p_{1/2}$ ,  $0g_{9/2}$ ,  $0g_{7/2}$ ,  $1d_{5/2}$ ,  $1d_{3/2}$ ,  $2s_{1/2}$ ,  $0h_{11/2}$  allowing

$J^\pi$	$E_x$ (keV)	Calculated $E_x$ (keV)	$I_\beta$ (%)	$\log ft$	Calculated $\log ft$
(7/2 <sup>+</sup> )	252.9(5)	219.0	< 54(4)	> 5.16(9)	6.0708
(9/2 <sup>+</sup> )	891.9(5)	974.0	< 35(3)	> 5.12(9)	6.1870
(11/2 <sup>+</sup> )	1144.5(5)	1055.0	< 11(2)	> 5.55(9)	6.2758

**Table 2.**  $I_\beta$  assigned to  $^{101}\text{Cd}$  levels. The following quantities are listed: the spin-parity of the level ( $J^\pi$ ), the energy of the initial level ( $E_x$ ), its  $\beta$  intensity ( $I_\beta$ ),  $\log ft$  value and  $\log ft$  value obtained with shell-model calculations.

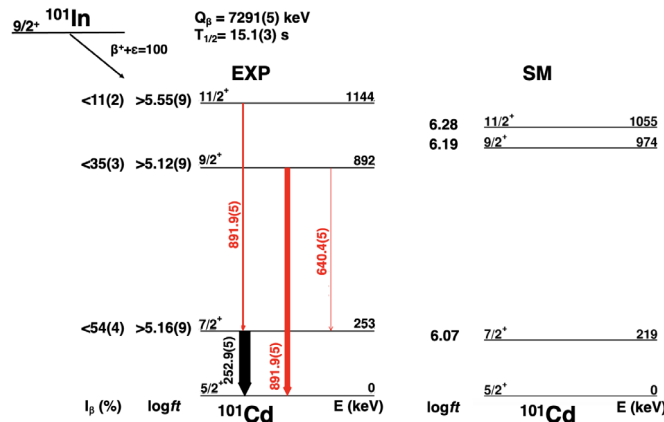


**Figure 2.** Decay scheme of  $^{101}\text{Cd}$  obtained in this work (left panel), the level scheme obtained in the theoretical calculation is displayed in blue (right panel).

for one-particle-one-hole excitations between two major shells. The single particle energies of the Hamiltonian are set considering a  $^{90}\text{Zr}$  core [17]. The nucleon-nucleon interaction used in the  $f5pg9$  model space is the JUN45 interaction [18], while the neutron-neutron interaction in the  $g7dsh11$  shell and the proton-neutron interaction across two major shells are derived from the monopole based universal interaction (VMU) [19, 20].

The aforementioned results are summarised in the proposed level scheme in Fig. 2, where transitions newly added to the  $\beta$ -delayed scheme are shown with red arrows and theoretical predictions are displayed in the right panel. The spin and parity of the  $^{101}\text{Cd}$  ground state has been fixed by a collinear laser experiment to  $J^\pi = 5/2^+$  [4], ruling out the direct ground-state-to-ground-state feeding from the  $J^\pi = 9/2^+$  ground state of the parent nucleus. The extracted  $I_\beta$  values suggest a strong feeding to the first three excited states, thus supporting the proposed spin and parity assignments as  $7/2^+$ ,  $9/2^+$  and  $11/2^+$ , given an allowed character of the transitions. The  $\log ft$  values obtained in this work are consistent with allowed  $\beta$  decay. The calculated values point to a similar feeding pattern, describing the transition as a proton in the  $0g_{9/2}$  shell being converted into a neutron placed in the  $0g_{7/2}$  shell in the daughter nucleus.

As a conclusion, our results point at allowed  $\beta$  decay transitions in  $^{101}\text{Cd}$  for the populated excitation levels. An allowed decay scheme is also consistent with large scale shell-model calculations for the given nucleus performed by C. Yuan et al. [17]. The spin-parity of the measured levels suggested by previous works is confirmed by this study.

## Acknowledgements

The authors would like to acknowledge the excellent work of the local HISPEC-DESPEC, FRS groups and accelerator teams. The results presented here are based on the experiment S496, which was performed at the DESPEC decay station at the GSI, Helmholtzzentrum für Schwerionenforschung, Darmstadt (Germany) in the frame of FAIR Phase-0. Support is acknowledged to INFN.

## References

- [1] T.R. Rodríguez, J.L. Egido, A. Jungclaus, Phys. Lett. B **668**, 410 (2008). <https://doi.org/10.1016/j.physletb.2008.08.072>
- [2] T. Faestermann, M. Górska, H. Grawe, Prog. Part. Nucl. Phys. **69**, 85 (2013). [10.1016/j.ppnp.2012.10.002](https://doi.org/10.1016/j.ppnp.2012.10.002)
- [3] J. Park et al., Phys. Rev. C **99**, 034313 (2019). <https://doi.org/10.1103/PhysRevC.99.034313>
- [4] D.T. Yordanov et al., Phys. Rev. C **98**, 011303 (2018). <https://doi.org/10.1103/PhysRevC.98.011303>
- [5] H. Geissel et al., Nucl. Instrum. Methods Phys. Res., B **70**, 286 (1992). [https://doi.org/10.1016/0168-583X\(92\)95944-M](https://doi.org/10.1016/0168-583X(92)95944-M)
- [6] G. Münzenberg, Nucl. Instrum. Methods Phys. Res., A **70**, 265 (1992). [https://doi.org/10.1016/0168-583X\(92\)95942-K](https://doi.org/10.1016/0168-583X(92)95942-K)
- [7] A. Mistry et al., Nucl. Instrum. Methods Phys. Res., A **1033**, 166662 (2022). <https://doi.org/10.1016/j.nima.2022.166662>
- [8] O. Hall et al., Phys. Lett. B **816**, 136266 (2021). <https://doi.org/10.1016/j.physletb.2021.136266>
- [9] J. Simpson, Z. Phys. A **358**, 139 (1997). <https://doi.org/10.1007/s002180050290>
- [10] M. Rudigier et al., Nucl. Instrum. Methods Phys. Res., A **969**, 163967 (2020). <https://doi.org/10.1016/j.nima.2020.163967>
- [11] M. Palacz et al., Nucl. Phys. A **608**, 227 (1996). [https://doi.org/10.1016/0375-9474\(96\)00287-4](https://doi.org/10.1016/0375-9474(96)00287-4)
- [12] M. Huyse et al., Z. Phys. A **330**, 121 (1988). <https://doi.org/10.1007/BF01287275>
- [13] T. Kibédi et al., Nucl. Instrum. Methods Phys. Res., A **589**, 202 (2008). <https://doi.org/10.1016/j.nima.2008.02.051>
- [14] M. Emeric, A. Sonzogni, <https://www.nndc.bnl.gov/logft/>, <https://www.nndc.bnl.gov/logft/>
- [15] M. Mougeot et al., Nature Physics **17**, 1099 (2021). <https://doi.org/10.1038/s41567-021-01326-9>
- [16] J. Szerypo et al., Z. Phys. A **359**, 117 (1997). <https://doi.org/10.1063/1.57353>
- [17] C. Yuan (2022), private Communication
- [18] M. Honma, T. Otsuka, T. Mizusaki, M. Hjorth-Jensen, Phys. Rev. C **80**, 064323 (2009). [10.1103/PhysRevC.80.064323](https://doi.org/10.1103/PhysRevC.80.064323)
- [19] T. Otsuka, T. Suzuki, M. Honma, Y. Utsuno, N. Tsunoda, K. Tsukiyama, M. Hjorth-Jensen, Phys. Rev. Lett. **104**, 012501 (2010). [10.1103/PhysRevLett.104.012501](https://doi.org/10.1103/PhysRevLett.104.012501)
- [20] B. Cai, C. Yuan, G. Zhang, Y. Zhang, M. Liu, Y. Xing, X. Xu, J. Li, M. Wang, Phys. Rev. C **109**, L051302 (2024). [10.1103/PhysRevC.109.L051302](https://doi.org/10.1103/PhysRevC.109.L051302)